MISSIONE 4
ISTRUZIONE RICERCA

National Recovery and Resilience Plan (NRRP)

Mission 4, Component 2 (M4C2) – Investment 1.1: Fund for the National Research Programme (NRP) and Research Projects of Significant National Relevance (PRIN)

Call PRIN 2022 PNRR – Directorial Decree no.1409, 14/09/2022

Enhancing our understanding of Subsidence RISK induced by groundwater exploitation towards sustainable urban development

CUP: B53D23033400001

DEL 4.1

Static 3D model of a (multi)aquifer system underlying a metropolitan city in Italy. The Bologna case study

Authors: X. Tang, P. Teatini, C. Zoccarato (UNIPD), R. Bonì (IUSS), F. Cigna, R. Paranunzio (CNR-ISAC),

Version 1.0, Issue date: 31/07/2025

Dissemination level: Public

Finanziato dall'Unione europea NextGenerationEU | Ministero dell'Università e della Ricerca | Italiadomani | CNR ISAC | IUSS Scuola Universitaria Superiore Pavia | Università degli Studi di Padova

How to cite this document

TANG X., TEATINI P., ZOCCARATO C., BONÌ R., CIGNA F. & PARANUNZIO R. (2025). *PRIN 2022 PNRR SubRISK+ Deliverable DEL 4.1: Static 3D model of a (multi)aquifer system underlying a metropolitan city in Italy. The Bologna case study*, Version 1.0, Issue date: 31/07/2025, pp. 31. Public Report. Available at: https://www.subrisk.eu/deliverables

Acknowledgements

The authors would like to thank Dr. Andrea Chahoud, Dr. Marco Marcaccio and Dr. Marianna Mazzei of the ARPAE Emilia-Romagna, Dr. Paolo Severi, Dr. Luisa Perini and Dr. Lorenzo Calabrese of the Regione Emilia-Romagna for the provided datasets and fruitful discussions about the project outcomes.

Revision history

Revision no.	*Authors*	*Date*	*Description*
1.0	TANG X, TEATINI P., ZOCCARATO C., BONÌ R., CIGNA F., & PARANUNZIO R.	31/07/2025	First release

Executive summary

This report summarizes the first results of SubRISK+ Work Package (WP) n.4 (*WP4: Advanced Local Scale Modelling*). WP4 is aimed to 1) develop city-scale representative lithofacies model reflecting the high heterogeneity and uncertainty of o the aquifer system, 2) integrate the lithofacies model into a 3D fluid-dynamic model coupled with a 3D geomechanical model, 3) simulate land subsidence (and horizontal displacements) by the comprehensive modelling system, and 4) perform EO data assimilation with the aim to improve its capacity for land subsidence prediction over the next decades. The advanced modelling system is developed for the city of Bologna and its suburban area, the Italian metropolitan city where land subsidence has reached the highest values, up to 3.5 m over the period from 1900 to 2020 (Zuccarini et al., 2024), forcing regional and local authorities to take legislative measures aimed to control the process (law, 10 December 1980, n. 845). The subsidence rate is also today larger than 20 mm/year in some portions of the city (https://egms.land.copernicus.eu/).

The state-of-the-art modelling approach proposed in this study is aimed to account for the peculiarity of the Bologna case study and to respond to the SubRISK+ goals: a) the 3D approach, both for the flow and the geomechanical simulations, will allow the comprehensive quantification of differential displacements caused by groundwater withdrawal; b) the stochastic approach, both in terms of hydrogeological setting and parameters estimation, will allow the inclusion of the uncertainties related to the subsurface features of the Bologna metropolitan area in the modelling framework.

This DEL4.1 focuses on the set-up of the 3D static (i.e., lithostratigraphic) model of the city of Bologna using a lithofacies (i.e., stochastic) approach. The geological and hydrogeological datasets that provide conditional inputs for lithofacies simulations were obtained from the Emilia-Romagna Geoportal and the Regional Agency for Prevention, Environment and Energy of Emilia-Romagna (ARPAE). A total of 175 borehole logs are used as conditioning data for lithofacies simulations. The dataset is distributed over an area of roughly 120 km^2 encompassing the Bologna city centre and its suburban fringe. To capture the marked heterogeneity of the Bologna alluvial fan, more than one hundred stochastic realisations were carried out under identical parameter settings but with distinct random seeds.

Deliverable DEL4.1 presents the 3D lithofacies model for the city of Bologna, summarizing the available dataset and the implemented approach. We show how the 3D lithofacies model is subsequently integrated into a conforming finite-element (FE) mesh. Using the algorithm described in Section 3.1.1, we validated the model ability to reproduce the evident lithological heterogeneity documented by borehole logs across the Bologna study area. This integrated representation provides a robust foundation for the subsequent hydrodynamic and geomechanical simulations planned in the next phases of the work.

Contents

1. INTRODUCTION

SubRISK+: Enhancing our understanding of Subsidence RISK induced by groundwater exploitation towards sustainable urban development is a collaborative two years research project funded in 2023 in the framework of the Italian National Recovery and Resilience Plan (NRRP), Mission 4, Component 2 (M4C2) – Investment 1.1: Fund for the National Research Programme (NRP) and Research Projects of Significant National Relevance (PRIN) [Call "PRIN 2022 PNRR", D.D. no.1409, 14/09/2022], and led by the National Research Council (CNR) of Italy – Institute of Atmospheric Sciences and Climate (ISAC), in collaboration with the University School for Advanced Studies (IUSS) of Pavia – Department of Science, Technology and Society (STS), and the University of Padua (UNIPD) – Department of Civil, Environmental and Architectural Engineering (ICEA).

With reference to the city of Bologna, which has been selected as local hotspot for the SubRISK+ analyses at the local scale, this report (DEL4.1) summarizes the results of SubRISK+ Work Package (WP) n.4 (*WP4: advanced local scale modelling*), aimed to i) develop a 3D city-scale representative lithofacies model reflecting the high heterogeneity of soil distribution, ii) integrate the lithofacies model into a 3D finite element grid that will be used for fluid-dynamic geomechanical modelling analyses.

Deliverable 4.1 is structured as follows:

- section 2 describes the data available (section 2.1) and the methodology implemented (section 2.2) to develop a lithofacies model of the city of Bologna;
- section 3 presents the results in terms of 3D lithofacies simulations achieved through the software GEOST (Clarke & Fogg, 1996; Dai et al., 2005);
- section 4 summarizes the outcome obtained in terms of 3D finite element grid populated with facies-dependent hydraulic conductivity and compressibility field, which will be used by the fluid-dynamic and geomechanical simulators (FLOW3D and GEPS3D) (Teatini et al., 2006; Isotton et al., 2019).

2. DATA & METHODS

2.1. Input datasets

2.1.1. General context

The lithostratigraphical setting of the Bologna aquifer system has been defined based on available dataset provided by the regional authorities of the Emilia Romagna region. In complex depositional settings such as alluvial environments, the standard concepts of superposition and lateral continuity of strata are often violated, with lithostratigraphic correlation that is challenging even over short distances. Indeed, the abrupt or transitional lateral facies changes due to the presence of different depositional domains leads to considerable uncertainty in the final geological model. Therefore, in such cases, lithofacies analysis provides a more robust categorisation of subsurface geological units as lithofacies mainly reflect the depositional environments and processes, while their associations provide a reliable architecture of sedimentary bodies and their geometries.

The input datasets of the analysis include: (i) geological datasets of the Emilia-Romagna Region geoportal (https://geoportale.regione.emilia-romagna.it/download), (ii) the hydrogeological data provided by the Regional Agency for Prevention, Environment and Energy of Emilia-Romagna (Arpae), Italy (https://www.arpae.it/it/temi-ambientali/acqua/dati-acque/acque-sotterranee/rete-di-monitoraggio-acque-sotterranee/il-monitoraggio-quantitativo-delle-acque-sotterranee).

Moreover, a fundamental contribution is represented by the paper after Giacomelli et al. (2023). The authors re-interpreted 940 existing borehole logs, leading to a detailed reconstruction of the subsurface depositional architecture of the Bologna aquifer system. Their analysis revealed the presence of three distinct depositional domains (Figure 1) with different stratigraphic architectures. From west to east: Domain A (Reno River) corresponds to the gravel-dominated fill of a river valley abruptly passing to Domain B (Bologna urban area) that represents a morphological and stratigraphical divide, topographically elevated with respect to the surrounding areas and characterised by fine-grained deposits with frequent paleosols. Lastly, Domain C (Savena River) exhibits the typical alluvial fan pattern, marked by a gentle convex-up surface morphology with gravelly-sandy deposits with a low degree of lateral amalgamation.

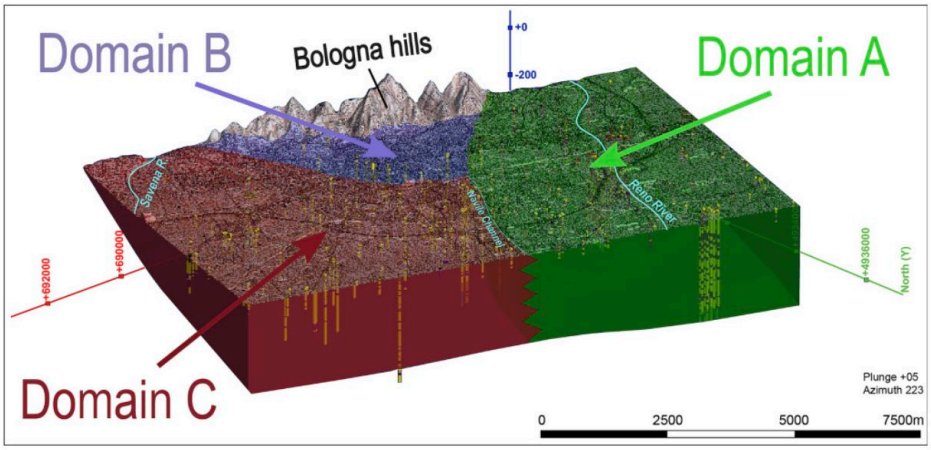

Figure 1 – A 3D view of the Bologna area showing the three domains that characterize the geological setting (source: Giacomelli et al., 2023).

2.1.2. Geographical and geological setting of the Bologna study area

Bologna is underlain by a thick succession of Quaternary alluvial deposits, which constitute a significant portion of the sedimentary infill of the Po Basin. Located at the foothills of the northern Apennines, the city occupies the coalesced alluvial fans formed by the Reno and Savena rivers (Teatini et al., 2006; Giacomelli et al., 2023).

The study area, encompassing both the historic city centre and its suburban surroundings, is bounded by the Bologna Hills to the south, the Reno River alluvial fan to the west, a distal fan plain to the north, and the Savena River alluvial fan to the east. It is noteworthy that the study area in Giacomelli et al. (2023) covers approximately 90 km². To mitigate potential boundary effects in our finite element modelling as discussed in Section 2.2.2, the model domain in this study has been expanded to approximately 120 km², with 14 km in length and 9 km in width (Figure 2). In the meanwhile, surface elevation declines from about 240 m above msl in the Bologna Hills to around 20 m above msl in the north-western corner (Figure 3).

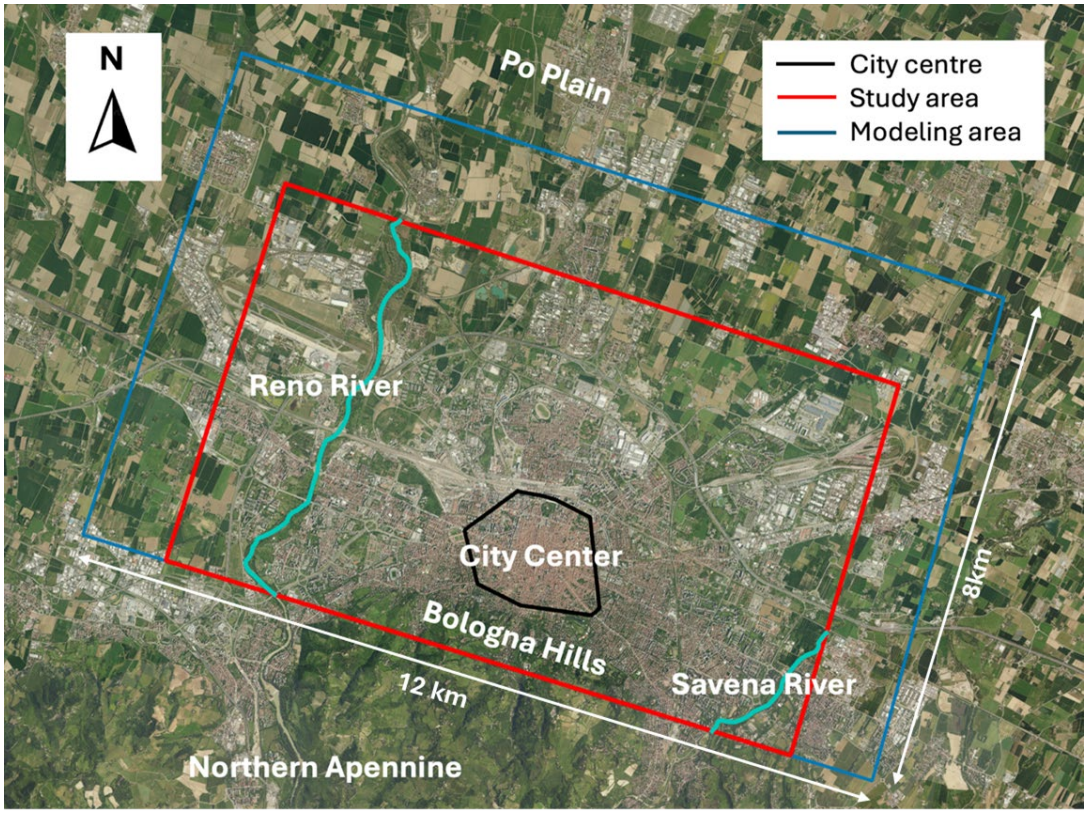

Figure 2 – Study area of Bologna, with the traces of the main watercourses and the Bologna city center.

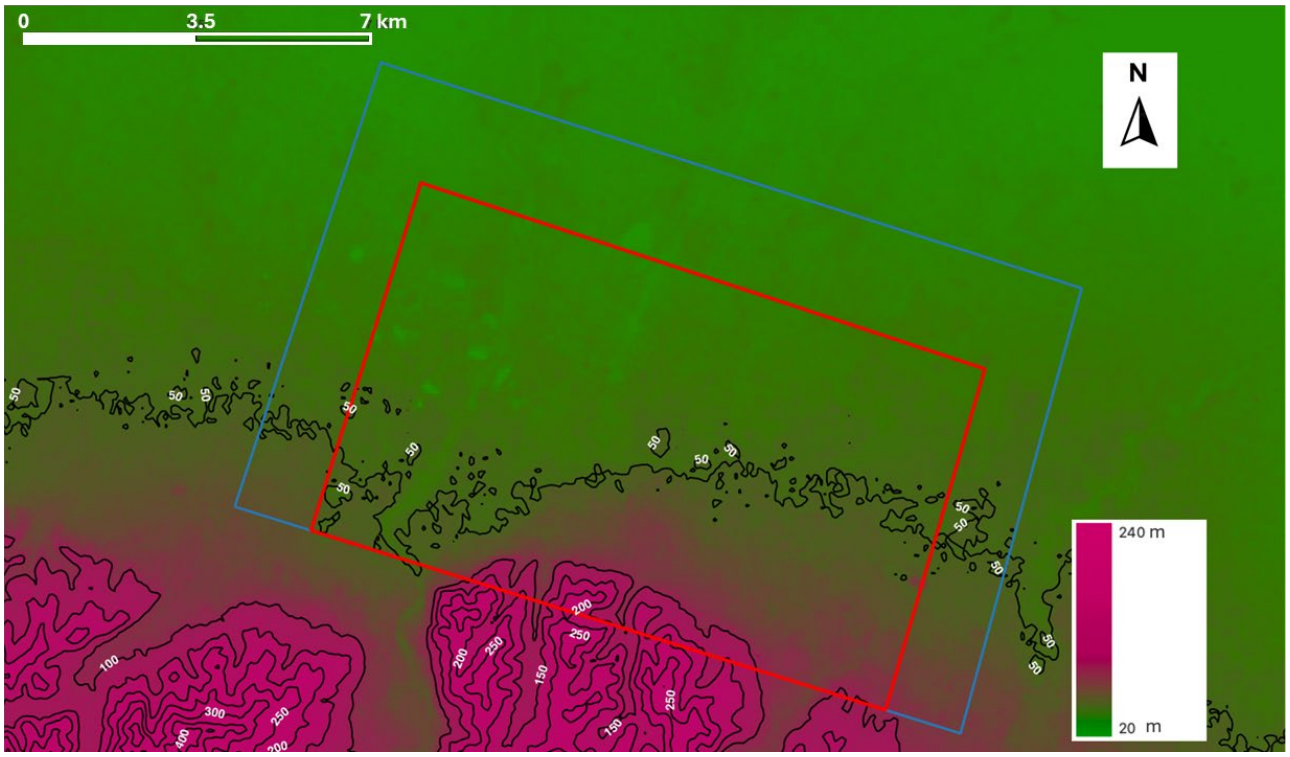

Figure 3 – Digital Elevation Map of Bologna (in m above msl). Source: Altimeter Corrected Elevations, Version2, ACE2. https://cmr.earthdata.nasa.gov/search/concepts/C3550196830-ESDIS.html.

The shallow subsurface (up to ~300 m) is characterized by significant lithological variability. (Giacomelli et al., 2023). Figure 4a presents two stratigraphic sections, PP′ and DD′, traced from the northeast to the southwest across the Po River plain and developed by exploiting stratigraphic logs from boreholes. Section PP′ (Figure 4b) intersects the city centre, whereas section DD′ (Figure 4c) crosses the distal portion of the alluvial fan. Both sections show that gravel occupies a large proportion of the shallow succession, with particularly high percentages adjacent to the Reno River (the easternmost part) from the surface to the deepest investigated levels. Away from these zones, the lithofacies distribution becomes more discontinuous and spatially variable, indicating pronounced heterogeneity.

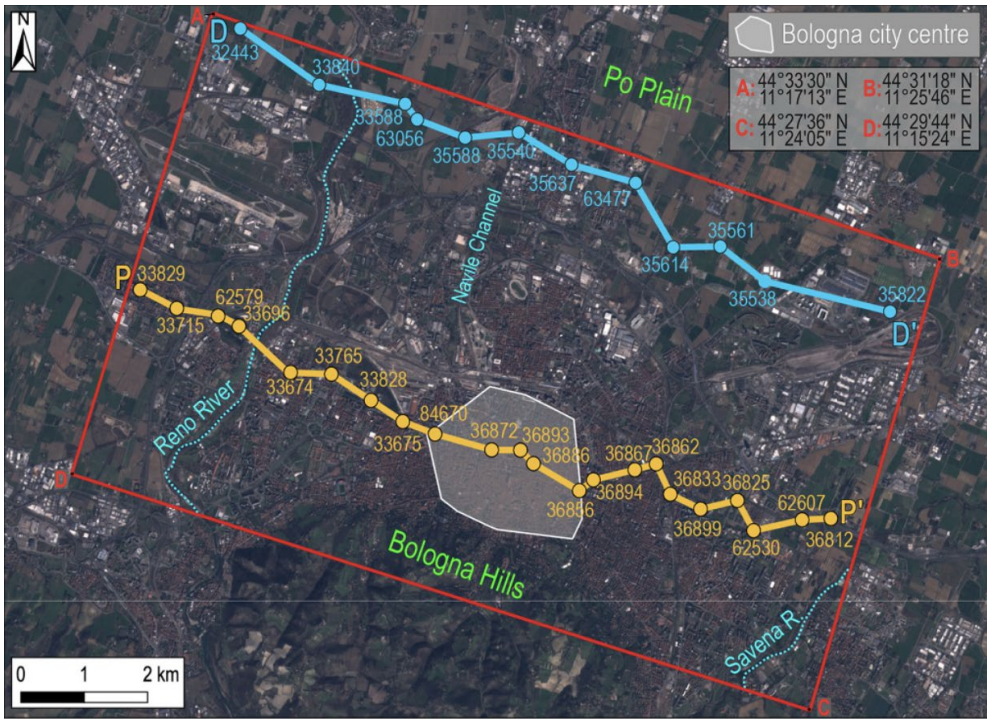

Figure 4 – a) Location of the stratigraphic cross-sections from northeast to southwest (source: Giacomelli et al., 2023)

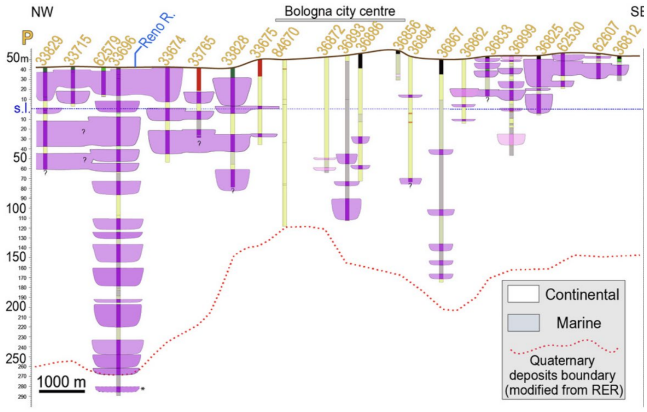

Figure 4 – b) Stratigraphic cross-section PP' crossing Bologna city centre (source: Giacomelli et al., 2023).

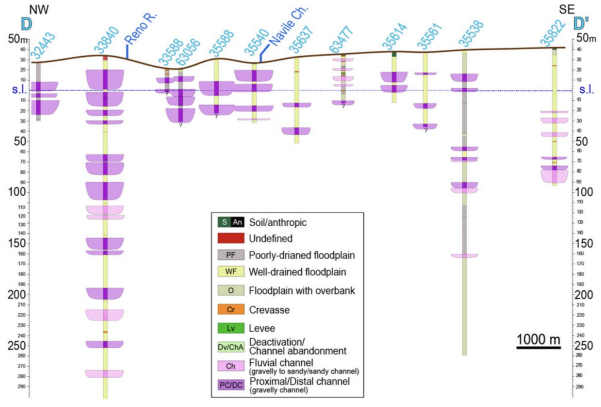

Figure 4 – c) Stratigraphic cross-section DD' crossing the distal part of the fan (source: Giacomelli et al., 2023).

Figure 5a shows the trace of three additional stratigraphic sections drawn from south to north. Section RR′ follows the Reno River, section MM′ extends from the Bologna foothills through the city centre to the distal alluvial fan, and section SS′ begins at the Savena River and continues toward the distal fan. Section RR′ (Figure 5b) exhibits a consistently high proportion of gravel in the shallow subsurface, consistent with the pattern observed in Figure 4b. Section MM′ (Figure 5d) does not display a distinctive facies arrangement; gravel occurs near both the top and the base, but its overall proportion is modest. Section SS′ (Figure 5c) shows a slightly elevated gravel content near the surface at its upstream end, but this tendency diminishes toward the distal fan. In the distal part of SS′, gravel also appears in deeper horizons, although it is intermixed with other lithofacies.

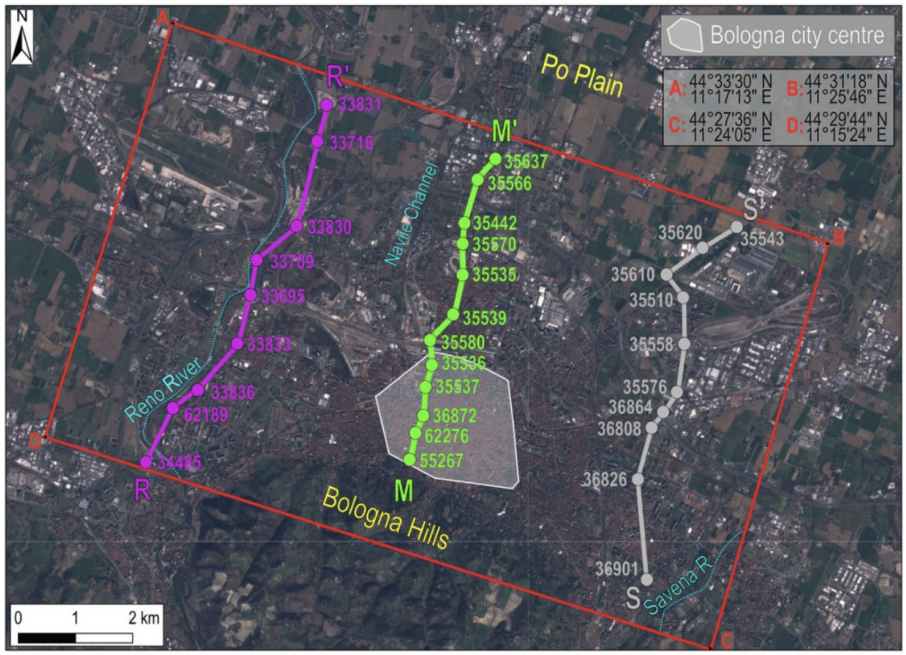

Figure 5 – a) Location of the stratigraphic cross-sections from south to north (source: Giacomelli et al., 2023).

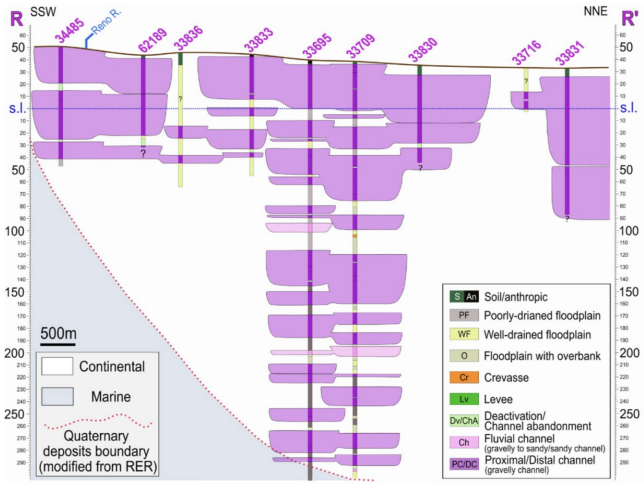

Figure 5 – b) Stratigraphic cross-section RR' along the Reno river (source: Giacomelli et al., 2023).

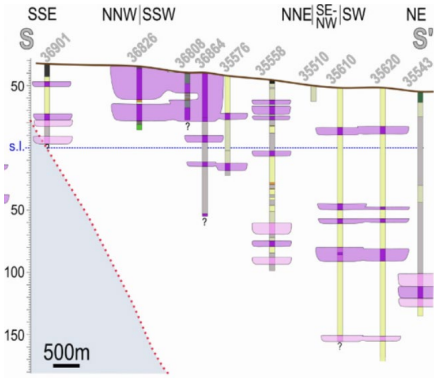

Figure 5 – c) Stratigraphic cross-section SS' from the Savena river to the distal portion of the alluvial fan (source: Giacomelli et al., 2023).

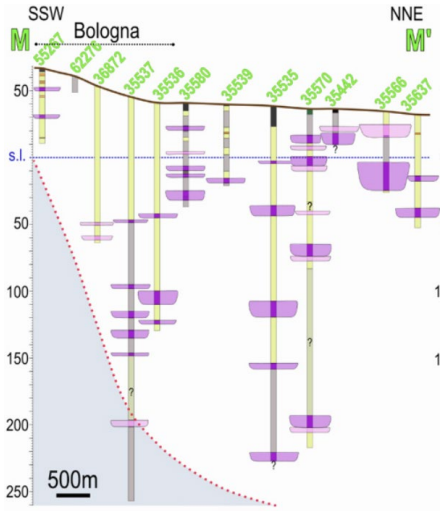

Figure 5 – d) Stratigraphic cross-section MM' crossing the Bologna city center (source: Giacomelli et al., 2023).

The boundary between Quaternary continental and marine deposits shown in figures 3b, 3c and 3d, was detected from geophysical surveys (i.e. Horizontal to Vertical Spectral Ratio measurements).

To address spatial complexity, the study domain was partitioned into three morpho-geological zones on the basis of surface morphology and depositional setting. Interpretation of 175 borehole logs (Figure 6) guided this subdivision, producing the three subdomains shown in Figure 7: Zone A, Zone B, and Zone C. Zone A is dominated by gravel, whereas Zones B and C display a more discontinuous distribution of lithofacies. This zoning framework provides the foundation for the probability-based statistical lithofacies simulation described in the following section.

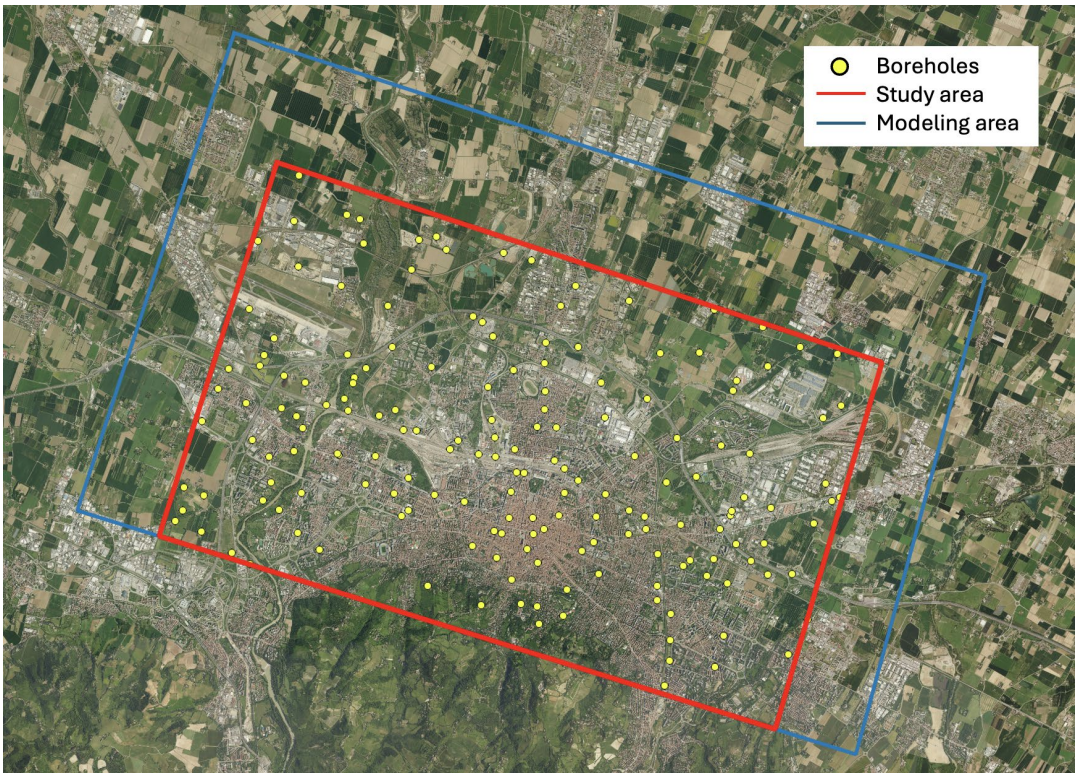

Figure 6 – Boreholes distribution in the study area. The stratigraphic profiles are available from the Emilia-Romagna Region geoportal.

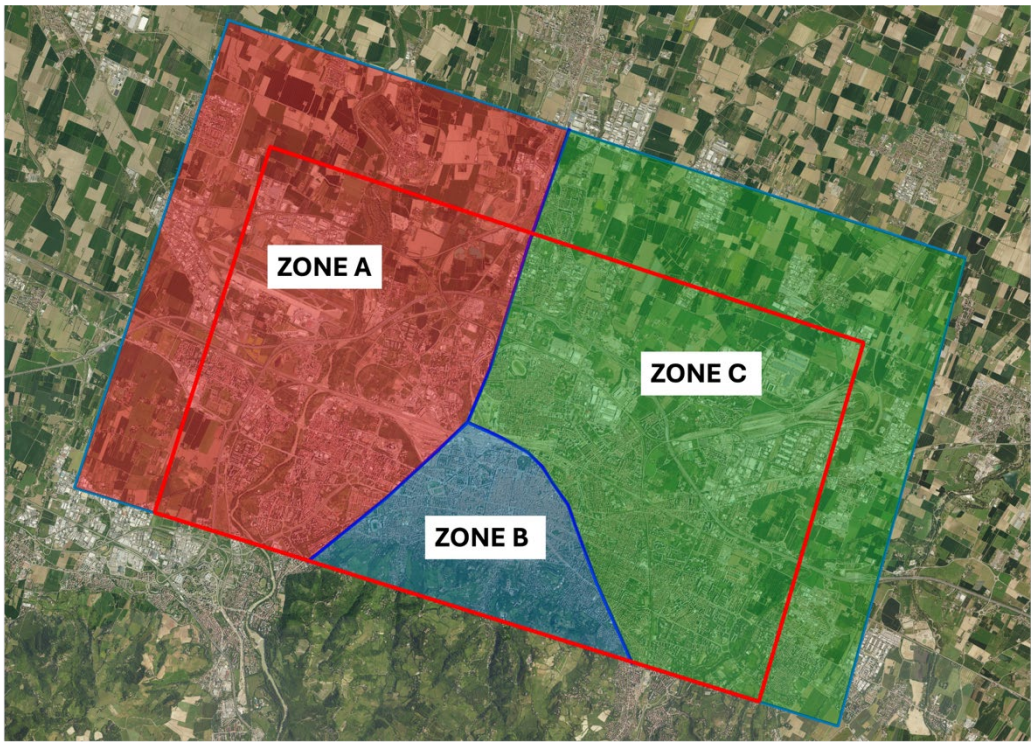

Figure 7 – Subdivision of the study area displaying the distinction of the three geological domains. From east to west: the Savena alluvial fan (green block-Domain C), the Bologna relief (purple block-Domain B), and the Reno River (red block-Domain A).

2.2. Methodologies

2.2.1. Multizone simulations of the 3D alluvial fan at Bologna

One of the critical factors influencing the accuracy and reliability of land subsidence simulations is the spatial distribution of subsurface lithofacies. This importance arises from the distinct mechanical properties and deformation responses exhibited by different soil types under groundwater extraction.

However, within the Bologna study area, the geomorphological framework of the alluvial plain exhibits a significant heterogeneity in shallow stratigraphy, leading to substantial variability in soil composition even over short spatial distances. As shown above, borehole investigations have enabled the identification of three distinct lithofacies zones (Zone A, Zone B, and Zone C), classified according to the predominant lithological composition observed within each zone (Giacomelli et al., 2023).

Although the soil lithology across the study area can be subdivided into numerous types from a purely sedimentological perspective (Figure 8), we have simplified this variability into four primary lithofacies based on their hydro-geomechanical properties: clay, silty clay, sand, and gravel. Lithofacies definition is the following:

1. “Clay”: poorly-drained fine-grained soil, light to dark, mostly soft clay;

2. "Silty-clay": well-drained fine-grained soil, yellowish to brownish, mostly stiff, clay as well as clay deposits characterized by silty and/or sandy formations;
3. "Sand": sandy soil: fine sand to coarse sand;
4. "Gravel": gravel to sand and gravelly deposits.

Accordingly, the lithofacies are grouped into these four classes for the purposes of this study. In Zone A (the Reno Domain), gravel is the predominant lithofacies, accounting for approximately 60% of the total volumetric proportion. In Zone B (the Bologna Domain), approximately 50% of the deposits consist of silty clay. Finally, Zone C (the Savena Domain) exhibits a considerably higher degree of heterogeneity compared to the other domains, with the volumetric proportions of the four lithofacies ranging from 10% to 40%.

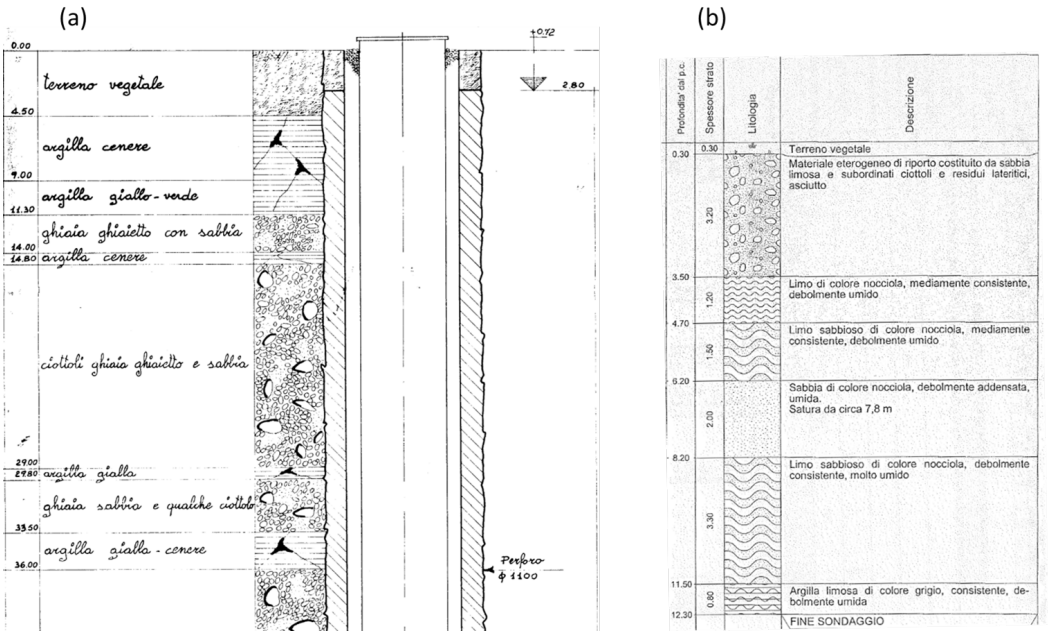

Figure 8 – Typical lithostratigraphic information available from the geological datasets of the Emilia-Romagna Region geoportal: (a) deep boreholes (down to 400 m depth below msl) and (b) shallow data from core drillings and CPT tests (tens of meters depth).

To address the challenge of reproducing the pronounced lithofacies heterogeneity across the Bologna study area, a multizone simulation is required to obtain a more statistically representative lithofacies distribution across the three domains. Accordingly, we adopt the multizone transition probability method developed by Zhu et al. (2016). Based on the consideration that the stationarity for a whole alluvial fan is typically tenuous (Weissmann & Fogg, 1999), the multizone transition probability method was used to preserve the local stationarity assumption of the system. Indeed, a large-scale fan can be divided into a number of zones characterized by stationary features, according to the geostatistical analysis of facies distributions.

The transition probability is the probability of sedimentary facies transition at different lag distances within a 3-D domain. By incorporating facies spatial correlations, volumetric proportions, and juxtaposition tendencies into a spatial continuity model, Carle & Fogg (1996) and Ritzi (2000)

developed transition probability models for aquifer characterization. Dai et al. (2007) proposed the following analytical solution $t_{ki}(h_\phi)$ for the transition probability model:

$$t_{ki}(h_\phi) = p_k + (\delta_{ki} - p_k)\, exp\,(-\frac{h_\phi}{\lambda_\phi}) \qquad (i = 1, 2, \dots, N; k = 1, 2, \dots, N)$$

where:

- $t_{ki}(h_\phi)$ is the transition probability from facies k to facies i along the ϕ direction with a lag distance h
- p_k is the volumetric proportion of facies k
- δ_{ki} is the Kronecker delta
- λ_ϕ is the integral scale in the direction of ϕ
- N is the number of input lithofacies

The borehole hydrofacies indicator data are processed by the geostatistical tool GEOST, developed by Dai et al. (2014) starting from the Geostatistical Software Library (Deutsch & Journel, 1992) and T-PROGS (Carle & Fogg, 1996), in order to compute the sample transition probabilities. GEOST is used for inversion of the multizone transition probability models. The parameters in equation (1) are optimally inverted through the modified Gauss-Newton-Levenberg–Marquardt method (Dai et al., 2008), with the prior information incorporated into the objective function as "conditional data" and used to define initial values, and minimum and maximum bounds. The 95% confidence intervals are also computed during the optimization process to quantify the uncertainty of estimated facies parameters. According to Zhu et al. (2016), the transition probability models for different zones, analyzed through indicator geostatistical simulations, can be used to represent the multizone architectures of the hydrofacies in the alluvial fan.

2.2.2. From 3D lithofacies grids to 3D finite element meshes

Modelling spatial and temporal evolution of piezometric head and land displacements requires the domain discretization into a 3D finite element mesh. The FLOW3D and GEPS3D simulators developed at the University of Padova (Isotton et al., 2019), and already applied in various cases worldwide (e.g., Ochoa-Gonzalez et al., 2018; Ye at al., 2018; Zhu et al., 2020), will be used in the next phase for the purpose.

The 3D (tetrahedral) mesh was developed starting from a two-dimensional (triangular) finite element mesh initially generated using Gmsh, an open source 3D finite element mesh generator with a built-in CAD engine and post-processor (https://gmsh.info/), and subsequently extended along the vertical direction using Gen3D, a specific software developed by the University of Padova.

The use of a tetrahedral finite elements, together with the stochastic approach implemented to describe the Bologna subsurface, has required the development of a specific procedure enabling the transformation of the discrete-point grid outputs obtained from GEOST into the continuous finite element mesh framework, thereby providing the computational foundation required to numerically solve the relevant partial differential equations.

Each tetrahedral element comprises four nodes; their x and y coordinates were averaged to locate the centroid, stored as $X_{c,i}$ and $Y_{c,i}$. For every layer the Euclidean distance between each lithofacies grid

node and the centroid of every tetrahedron was calculated. Whenever a shorter distance was identified, both the distance and the corresponding lithofacies class were updated.

Iterating through all nodes ensured that the minimum distance for each element was found, after which the associated lithofacies code was assigned to that element. Repeating this procedure across all layers provided lithofacies attributes for the entire mesh, thereby completing the coupling of the stochastic geological model with the static finite element discretisation. Below the algorithms have summarised the key ideas for this process.

Algorithm 2 Find and Store the Centroid of Tetrahedron.

for $i = 1, \ldots,$ total number of tetrahedrons **do**
  for $n = 1, \ldots, 4$ **do**
    $X_{n,i} =$ X coordinate of node n
    $Y_{n,i} =$ Y coordinate of node n
  end for
  $X_{c,i} = \sum_{n=1}^{4} X_{n,1}/4$
  $Y_{c,i} = \sum_{n=1}^{4} Y_{n,1}/4$
end for

Algorithm 3 Search for the Nearest Facies

for $i = 1, \ldots,$ number of lithofacies points at each layer **do**
  $\mathrm{xf}_i =$ x coordinate of facies at layer i
  $\mathrm{yf}_i =$ y coordinate of facies at layer i
  distance $= \sqrt{(X_{c,i} - \mathrm{xf}_i)^2 + (Y_{c,i} - \mathrm{yf}_i)^2}$
  if distance $<$ distance at the previous step **then**
    update distance
  end if
end for

3. RESULTS

3.1. Stochastically simulated lithofacies models

Since the study domain comprises three zones, each dominated by distinct lithofacies, the volumetric proportion p_k varies accordingly. Consequently, the facies-transition probabilities also differ from one zone to another. Lithofacies heterogeneity decreases with depth: data from the Emilia Romagna Geological Survey highlights that the layering of the aquifer system is more continuous at depth (ISPRA, 2009; Martelli et al., 2017). Therefore, we further subdivide each zone at a depth of -150 m above msl, below which the mean horizontal correlation length of lithofacies increases markedly.

A numerical domain measuring 20 km × 20 km × 1100 m was established for the stochastic lithofacies simulations. The lithofacies nodes amount to 2'200'000; their distance is 200 m along the x and y directions and equal to 5 m along z. To accommodate the pronounced vertical contrast in heterogeneity, the domain was partitioned at -150 m into an upper and a lower interval, and identical simulation workflows were executed for each interval.

For the upper interval, three separate realizations were generated, each adopting one of the lithofacies-proportion scenarios listed in Table 1. The values of the integral scale λ in the 3 zones along the main directions are summarised in Table 2. To ensure continuity across internal zoning boundaries, the simulations were performed sequentially: Zone A was simulated first, its boundary facies were extracted, and these facies were imposed as conditioning data for the subsequent simulations of Zones B and C. The workflow was then repeated for the lower interval. In this case, the integral scale values derived from the available data are much larger, consistent with the greater homogeneity characterizing the aquifer system at depth (Table 2). The smaller values in the upper zones reflect the higher heterogeneity near the surface.

Of the 175 borehole logs available, 69 were selected as conditioning data for the Zone A simulation, which covers an area of 60.6 km². Lithofacies indicators were assigned at 1-meter depth intervals along each selected borehole, generating 6752 conditioning nodes in total. After completing the realization for Zone A, 3520 facies indicators located on the interface between Zones A and B were extracted and used as additional conditioning data for the Zone B simulation. Consequently, the Zone B model, occupying 13.4 km², was conditioned on 6816 facies indicators (comprising its borehole data together with the transferred boundary data). The same procedure was applied to Zone C: 6160 boundary indicators were transferred from Zone A, bringing the total number of conditioning nodes for Zone C to 15337 across an area of 67.8 km².

Upon completion of the six coupled simulations (three zones per two depth intervals), the realizations were mosaicked according to the three morpho-geological subdivisions delineated in Figure 7. All 175 borehole lithofacies indicator logs served as conditioning data and were processed with the geostatistical package GEOST (Dai et al., 2005). The resulting three-dimensional lithofacies model fills a computational box that measures 20 km by 20 km in plan view and extends for a depth range of 1100 m (between +300 to -800 m above msl). Figure 9 depicts this model as a cloud of discrete points.

	GRAVEL	SAND	SILTY CLAY	CLAY
ZONE A UPPER	0.635	0.037	0.239	0.089
ZONE A LOWER	0.399	0.066	0.264	0.271
ZONE B UPPER	0.107	0.101	0.523	0.269
ZONE B LOWER	0.026	0.066	0.286	0.622
ZONE C UPPER	0.213	0.132	0.455	0.200
ZONE C LOWER	0.128	0.136	0.480	0.256

Table 1. Proportion of four main facies volume in the three zones and the two depth ranges (upper: from the land surface to -150 m above msl; lower: from -150 m above msl to the basement) characterizing the Bologna aquifer system.

	GRAVEL	SAND	SILTY CLAY	CLAY
λ_x - ZONE A UPPER	1250	75	215	215
λ_y - ZONE A UPPER	2500	120	430	430
λ_z - ZONE A UPPER	15.8	3.5	7.6	6.2
λ_x - ZONE A LOWER	5000	2000	5000	5000
λ_y - ZONE A LOWER	5000	2000	5000	5000
λ_z - ZONE A LOWER	9.1	3.3	8.9	9.1
λ_x - ZONE B UPPER	500	500	1000	500
λ_y - ZONE B UPPER	250	250	500	250
λ_z - ZONE B UPPER	5.1	7.4	17.5	16.9
λ_x - ZONE B LOWER	2000	2000	2500	5000
λ_y - ZONE B LOWER	2000	2000	2500	5000
λ_z - ZONE B LOWER	1.7	3.0	13.5	36.8
λ_x - ZONE C UPPER	850	500	1800	900
λ_y - ZONE C UPPER	425	250	900	450
λ_z - ZONE C UPPER	7.0	7.3	14.3	12.9
λ_x - ZONE C LOWER	2000	2000	4500	5000
λ_y - ZONE C LOWER	2000	2000	4500	5000
λ_z - ZONE C LOWER	5.5	4.6	14.2	17.1

Table 2. Integral scale (m) of four main facies volume in the three zones and the two depth ranges (upper: from the land surface to -150 m above msl; lower: from -150 m above msl to the basement) characterizing the Bologna aquifer system. Directions x, y, z correspond to northwest to southeast, southwest to northeast, and vertical, respectively.

Because the lithofacies simulations were carried out within a stochastic transition probability framework, 100 independent realizations were produced under identical parameter settings but with distinct random seeds. The procedure was as follows: (1) the upper and lower sections of Zone A were each simulated one hundred times with GEOST; (2) for every realization, accuracy was evaluated by comparing simulated lithofacies at borehole coordinates with the conditioning logs (the highest accuracy ratio reached 87%); (3) the single realization with the highest accuracy was retained for each section; (4) lithofacies along the boundaries shared with Zones B and C were extracted from these two selected realizations and used as additional conditioning data for Zones B and C; (5) the

same selection procedure was repeated for Zones B and C, yielding the best fitting upper and lower depth intervals upon the 100 simulations; (6) the six selected results (upper and lower sections of Zones A, B, and C) were merged into one three-dimensional lithofacies model. This workflow produced the optimal model from the 100 simulations.

The highest accuracy ratio (acc_rate) is obtained by the following algorithm:

Algorithm 1 Determine the Accuracy

Load the simulated lithofacies matrix as A
for $i = 1, \ldots,$ total number of lithofacies **do**
    X_i = X coordinate of i^{th} lithofacies
    Y_i = Y coordinate of i^{th} lithofacies
    Z_i = Z coordinate of i^{th} lithofacies
    P_i = Facies of i^{th} coordinate
end for
Apply KDTree method to search the nearest point between A and input conditional data
Obtain n nearest points with corresponding coordinates and lithologies from conditional data
repeat_count = 0
length = total number of lithofacies
for $j = 1, \ldots, n$ **do**
    if P_j == facies of j^{th} conditional data **then**
        repeat_count = repeat_count + 1
    end if
end for
acc_rate = repeat_count/length

Figures 10 and 11 show two additional realizations that illustrate the representative variability among the simulations. The comparison of the independent realizations shows that most lithofacies are characterized by consistent spatial patterns, resulting from the strong conditioning imposed by the borehole data. The fraction of lithofacies that varies between realizations reflects the intrinsic stochastic variability of the simulation framework.

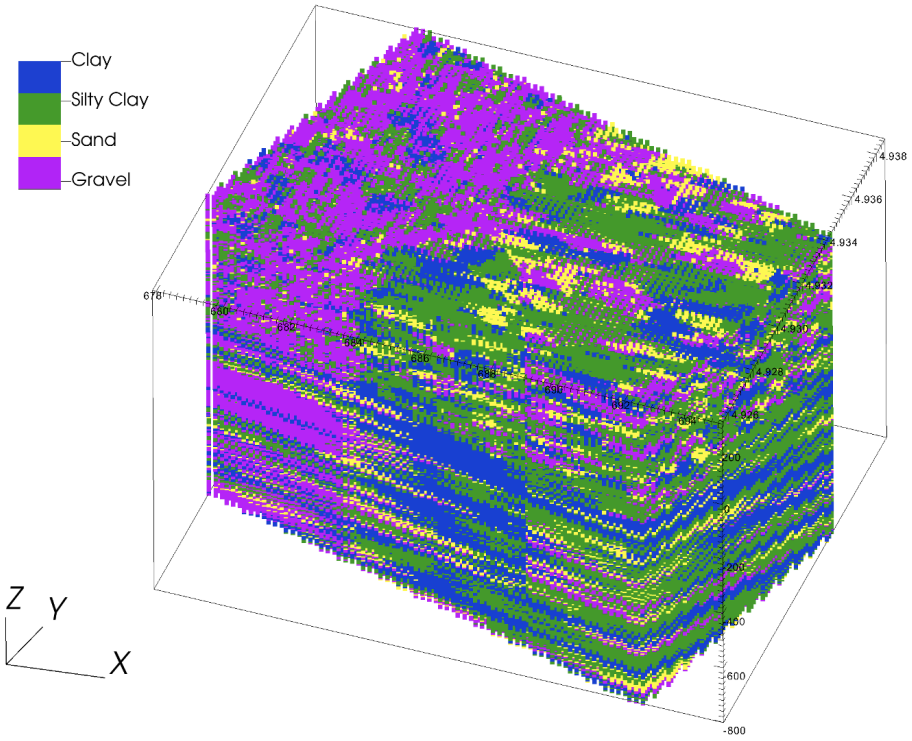

Figure 9 – Stochastically simulated lithofacies model #01. Vertical exaggeration is 10.

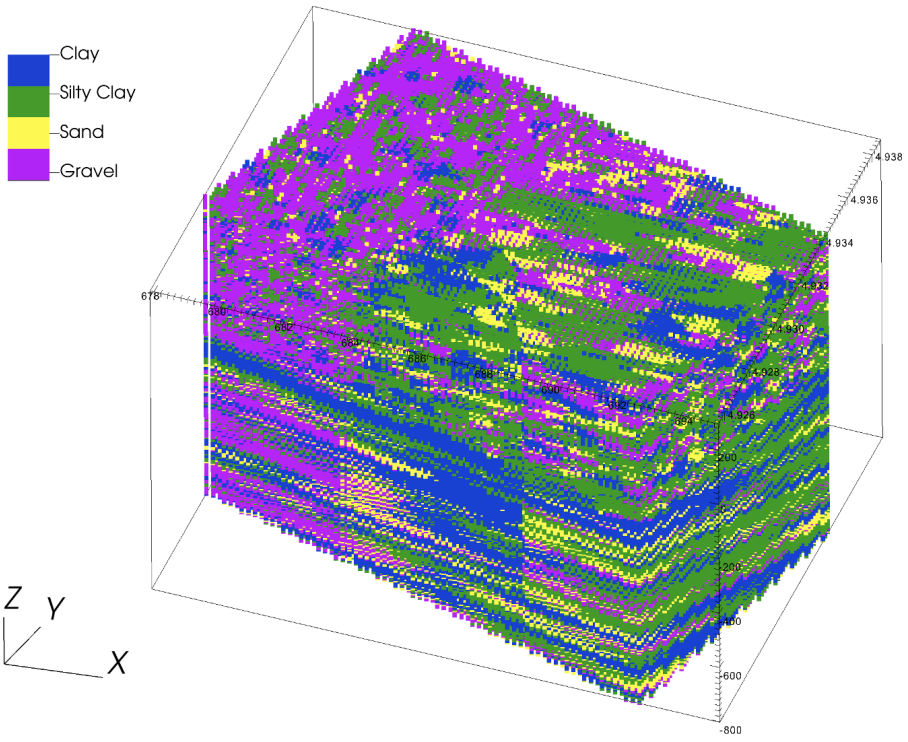

Figure 10 – Stochastically simulated lithofacies model #02. Vertical exaggeration is 10.

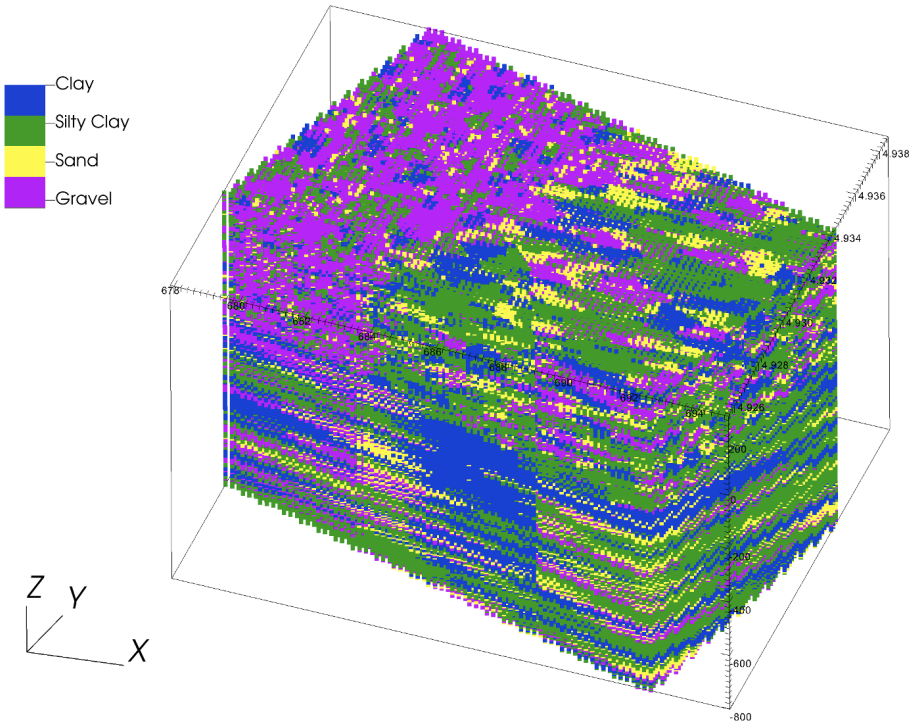

Figure 11 – Stochastically simulated lithofacies model #03. Vertical exaggeration is 10.

3.2. The 3D finite element mesh

Figure 12 depicts the planar finite element mesh that coincides with the modelling domain outlined in Figure 4b. The coordinates of the four corners defining the study area in Bologna were explicitly assigned within the modeling software. Furthermore, the mesh density was strategically refined in proximity to main wellfields and Bologna downtown, reflecting areas with heightened sensitivity and greater accuracy requirements for modeling land subsidence. The characteristic dimension of the triangles ranges from 80 m to 1000 m. The mesh is composed by 6'114 nodes that define 12'033 triangular elements, giving a total planimetric coverage of approximately 140 km². The characteristic dimensions of the triangles range from 80 to 1000 m, with the finer discretization adopted in Bologna downtown at in correspondence of the main wellfields.

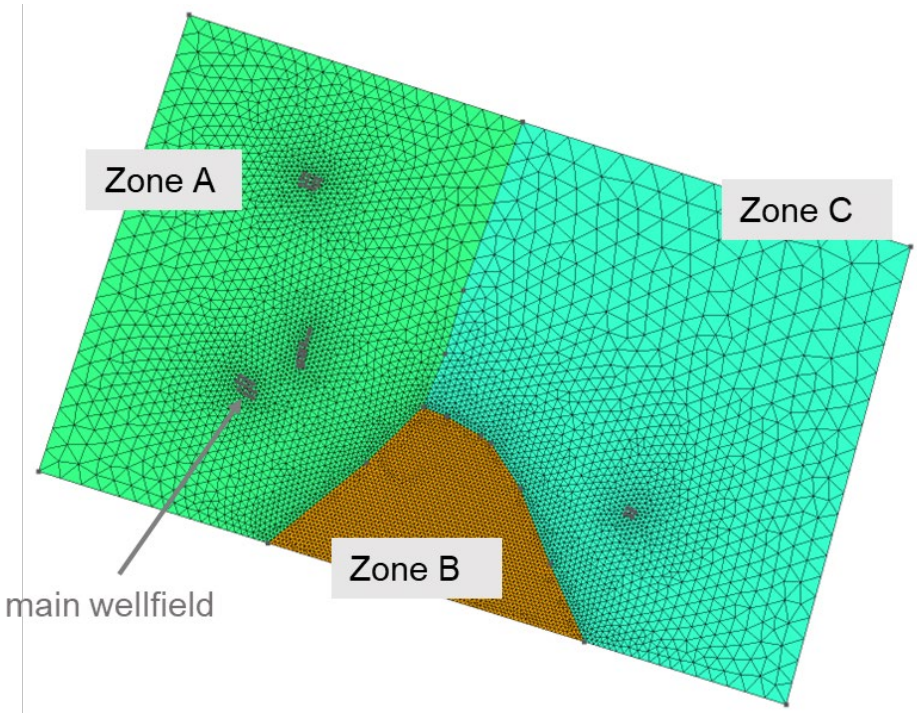

Figure 12 – The 2D finite element mesh of the study area. The three zones with different lithofacies structure are highlighted using different colours.

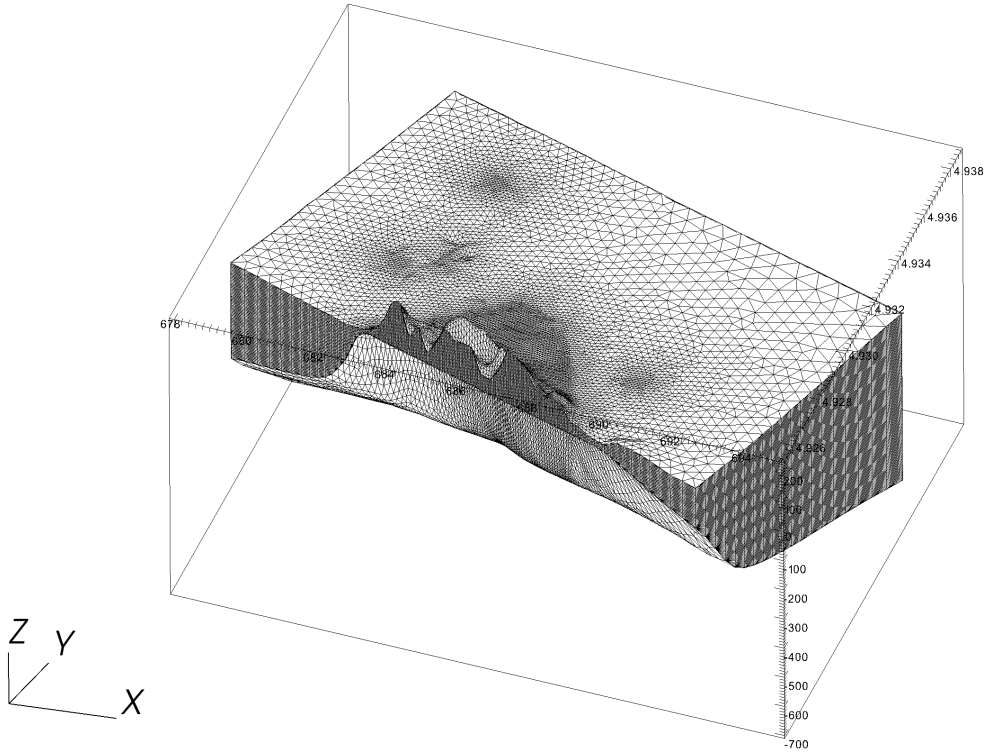

Figure 13 – The 3D finite element mesh of the study area. Vertical exaggeration is 10.

Based on the digital elevation model of the study area (Figure 3) and the bedrock depth derived from the geological information, the two-dimensional mesh was extruded vertically to generate a three-dimensional mesh. As illustrated in Figure 13, the bedrock surface dips from southwest to northeast because of the Apennine foothills. This surface will be treated in the dynamic modelling as impermeable and stable. Its depth ranges from 264 m above msl in the south to -708 m above msl to the north. The 3D mesh is made of 475'641 nodes and 2'673'410 elements, with 190 layers. The selected vertical discretization is 5 m, resulting from a balance between the expected CPU time required to run the models and the accuracy in the lithofacies representation.

Figure 14 illustrates an overlay of the static finite element mesh, prior to the assignment of lithofacies, with the stochastic lithofacies model generated by GEOST. Figure 15 displays the finite element mesh after the lithofacies classification has been incorporated, revealing the final spatial distribution within the numerical domain.

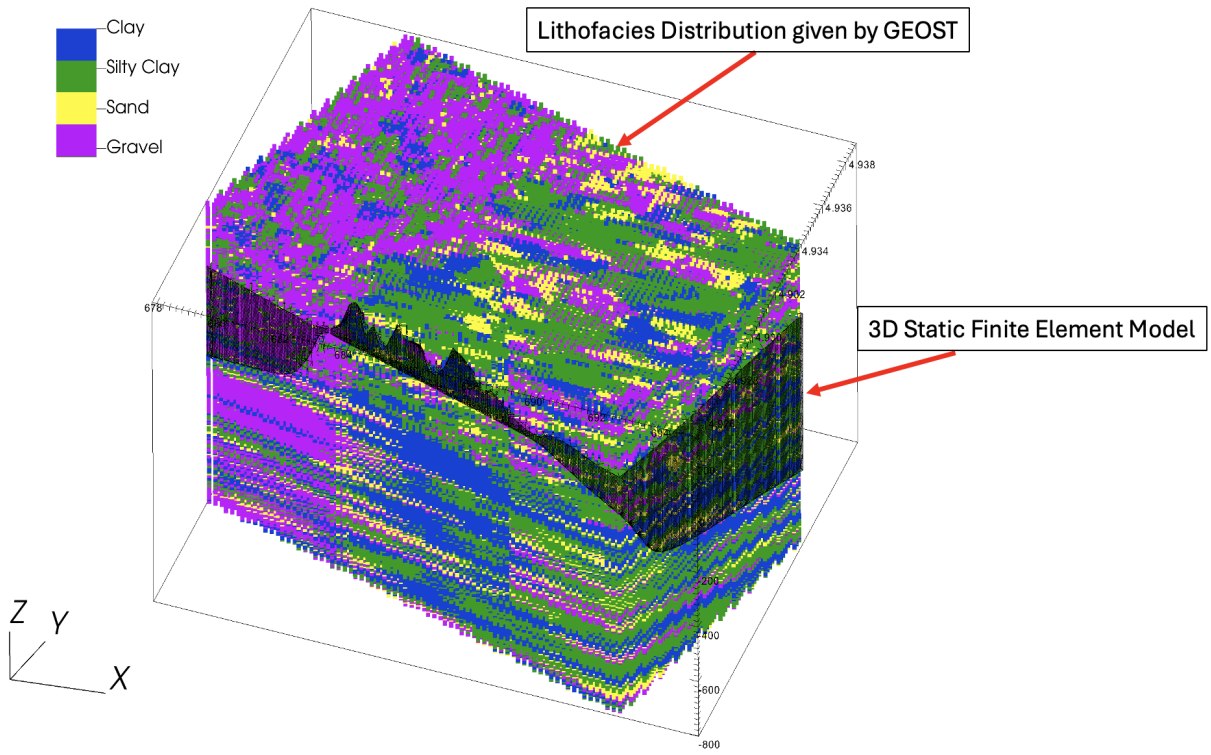

Figure 14 – Static finite element mesh overlapped to lithofacies model. Vertical exaggeration is 10.

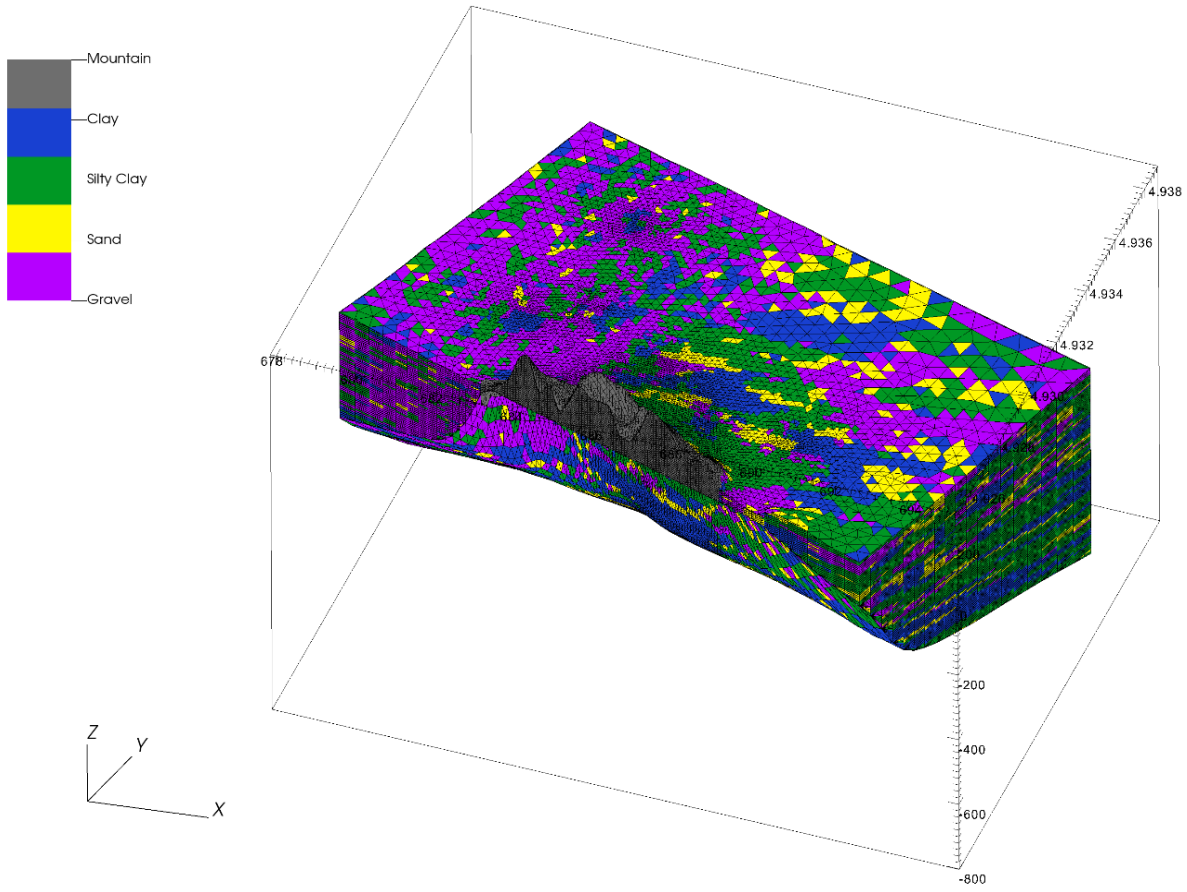

Figure 15 – Finite element model integrated with lithofacies distribution. Vertical exaggeration is 10.

As described above, a single lithofacies model is constructed from six simulations that account for variations in both lithofacies integral scale and facies proportion across each zone. Figure 16 show one of the facies outcome resampled on the 3D FE mesh where the two depth intervals characterized by different facies parameter are highlighted. As reported above, based on available lithostratigraphic sections (ISPRA, 2009; Martelli et al., 2017) the interface between the upper and lower portion was set at -150 m above msl, reflecting the point at which the horizontal correlation length of lithofacies becomes markedly larger. Consequently, the upper and lower portions of the 3D static model have different correlation lengths for the same lithofacies types, with a difference that amounts to more than 1 order of magnitude (Table 2).

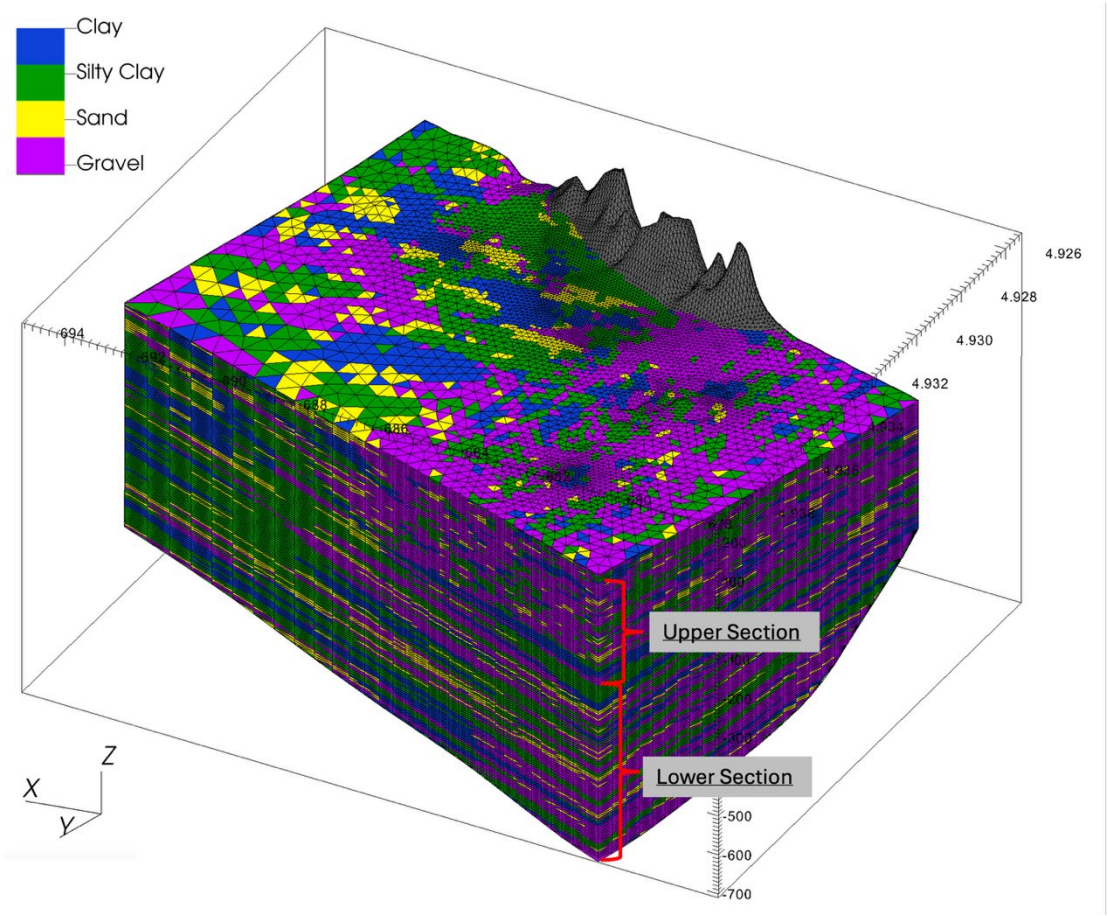

Figure 16 – Axonometric view of the finite element mesh with material distribution according to the facies realization #01. The two depth intervals with different parameter distributions are highlighted. Vertical exaggeration is 10.

A comparison between a vertical cross-section of a 3D static model and a hydrostratigraphic cross-section after ISPRA (2009) along the southwest to northeast direction is shown in Figure 17. The hydrogeological cross-section profile in Figure 17b shows that the main aquifer horizons, labelled A0 through A4, dip gently northward from the Apennine foothill toward the distal portion of the Bologna alluvial fan. To replicate this geometry, a preferential drift direction was specified in GEOST prior to the stochastic simulations. This drift aligns facies continuity with the observed structural dip, so the lithofacies assigned to the finite element mesh satisfactory mirrors the slope pattern documented by ISPRA (Figure 17a). This represents an important original update in the modelling framework.

Notice that the prevailing lithologies in Figure 17a are represented by fine deposits (clay and silty-clay) as the section is crossing Zone C.

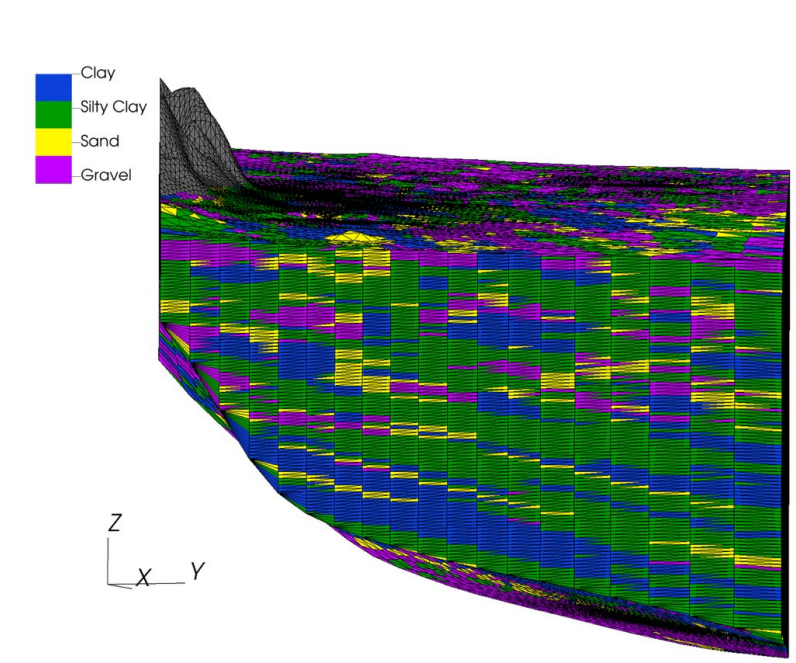

Figure 17 – a) Finite element model highlighting the dip angle.

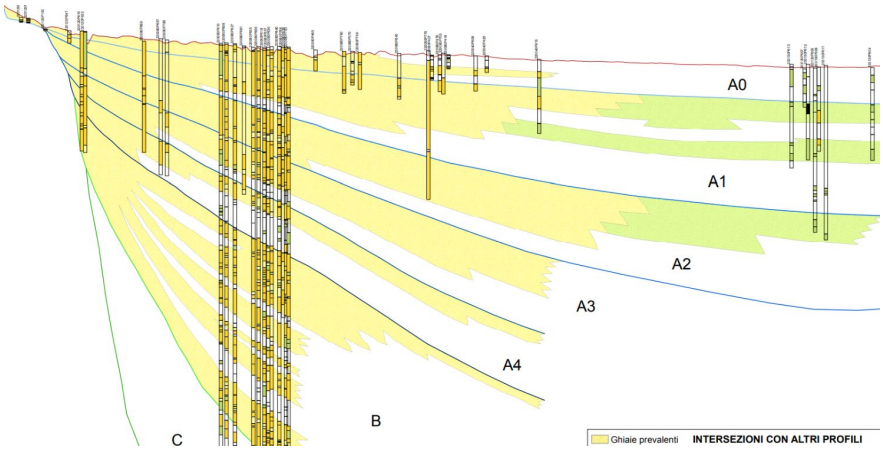

Figure 17 – b) Stratigraphic section of Bologna alluvial fan (after ISPRA, 2009)

Several sets of cross sections from the 3D FE model are presented in Figures 18 to 22 for three representative facies realizations generated with distinct random seed numbers. The section alignments coincide with those shown in Figure 4 and Figure 5. The comparison between the stratigraphic sections shown in Figures 4b and 4c and Figures 5b, 5c, and 5d (after Giacomelli et al., 2023) demonstrates that the FE model, once populated with lithofacies, reproduces satisfactorily the observed spatial distribution in the Bologna metropolitan area. For example, the sections in Figure 18 show a higher proportion of gravel in the area of the Reno River on the western side, shifting toward finer lithologies in the central portion and a more heterogeneous distribution to the east, in agreement with Figure 4b. Notice that in Figures 18, 19 and 20 vertical exaggeration is 10.

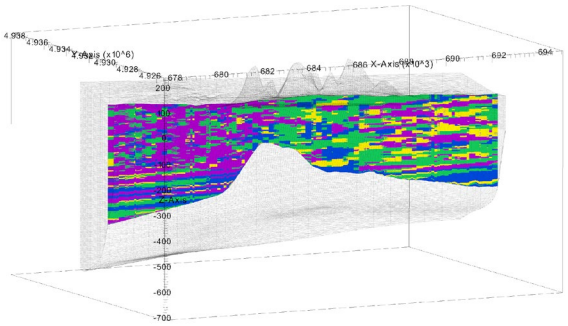

Figure 18 – a) PP' section from realization 1

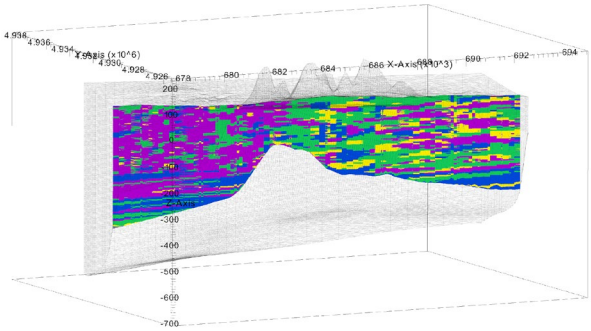

Figure 18 – b) PP' section from realization 2

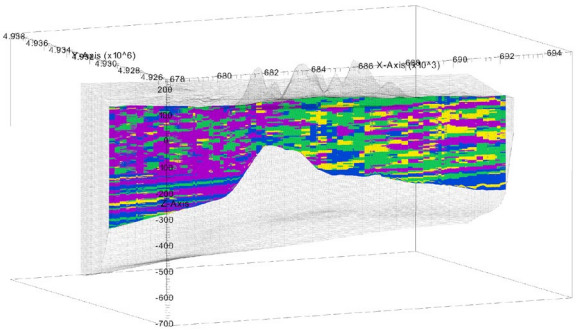

Figure 18 – c) PP' section from realization 3

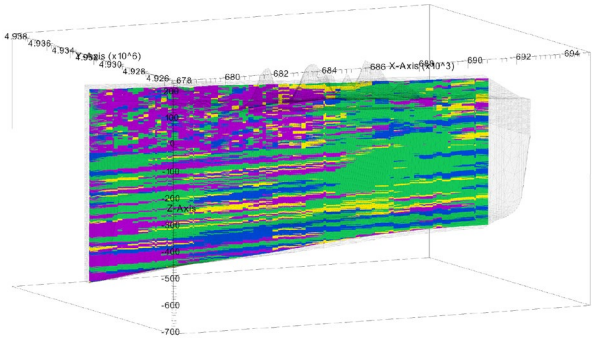

Figure 19 – a) DD' section from realization 1

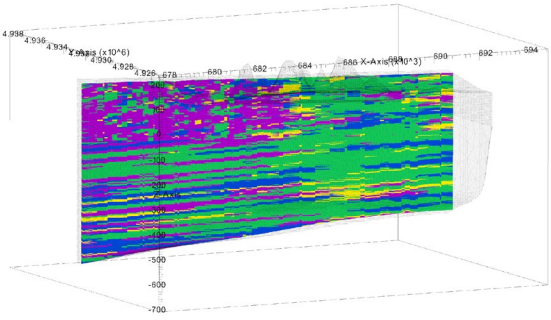

Figure 19 – b) DD' section from realization 2

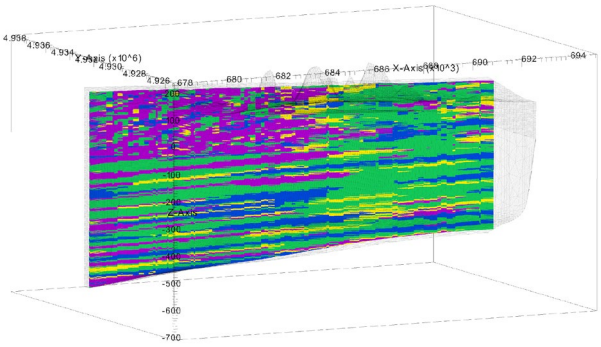

Figure 19 – c) DD' section from realization 3

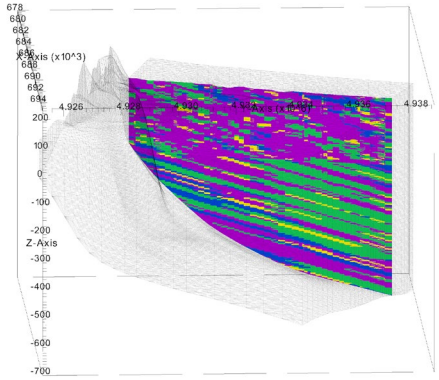

Figure 20 – a) RR' section from realization 1

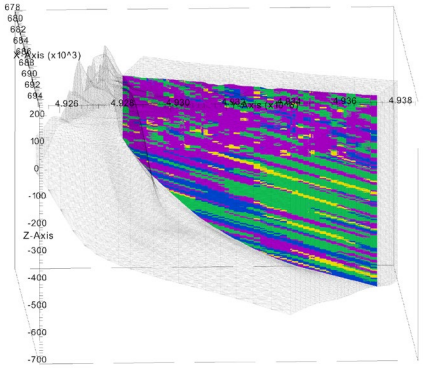

Figure 20 – c) RR' section from realization 3

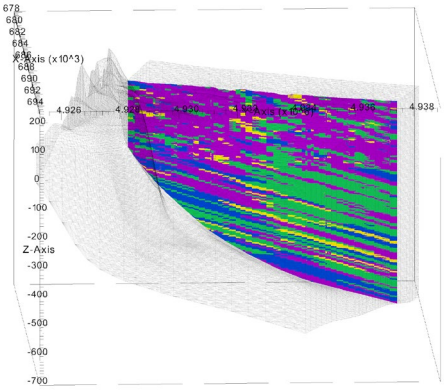

Figure 20 – b) RR' section from realization 2

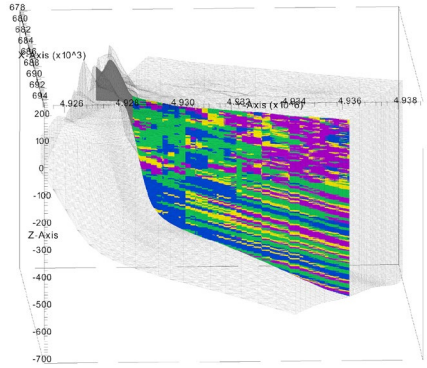

Figure 21 – a) MM' section from realization 1

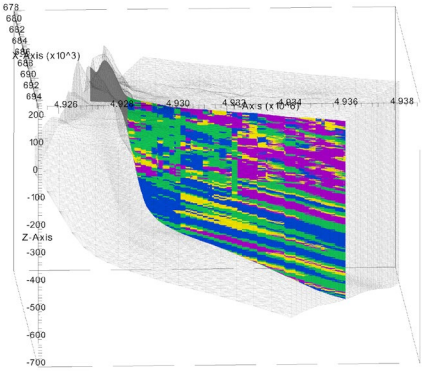

Figure 21 – c) MM' section from realization 3

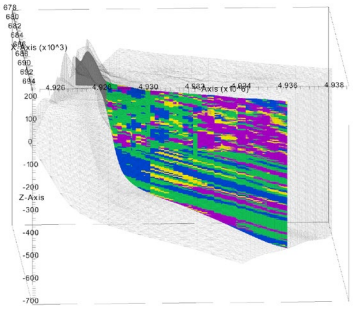

Figure 21 – b) MM' section from realization 2

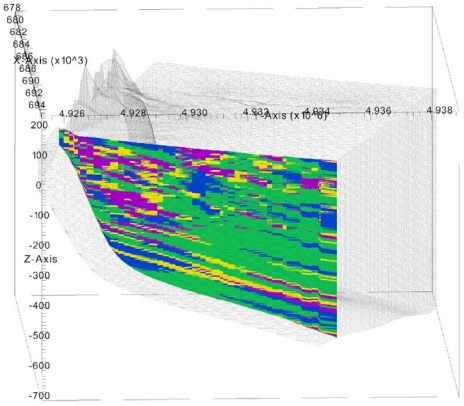

Figure 22 – a) SS' section from realization 1

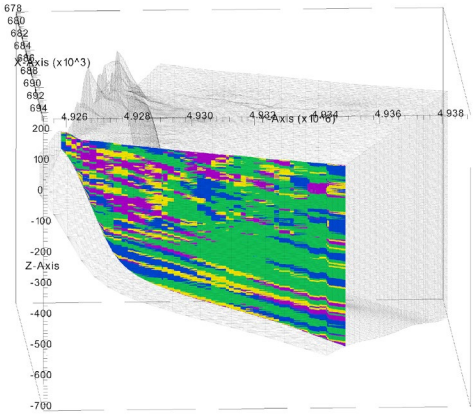

Figure 22 – b) SS' section from realization 2

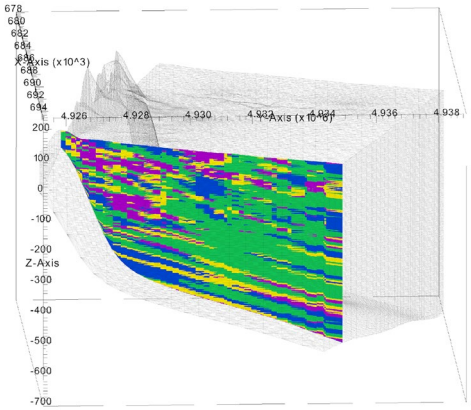

Figure 22 – c) SS' section from realization 3

4. CONCLUSIONS

The stratigraphic analysis of the Bologna metropolitan area reveals a highly heterogeneous alluvial architecture, which precludes the use of traditional modelling approaches that assume smoothly layered systems. By employing an advanced local scale modelling framework that combines a multi zone transition probability method with a three-dimensional finite element formulation, we were able to reproduce this complex lithofacies distribution using the lithological information from 175 borehole logs. The stochastic procedure generated six simulations (three for the upper depth interval and three for the lower depth interval) with different facies proportions and correlation lengths in the three Zones A, B, and C characterized by different sedimentation environments. Correlation lengths range from 100 m to 500 m in the upper depth interval and from 2000 m to 5000 m in the lower interval. The resulting lithofacies model was integrated into a finite element mesh of 20 km by 20 km by 1100 m, discretized into 189 layers with a 5 m vertical spacing. Centroid based matching ensured that each tetrahedral element inherited the closest lithofacies code from the stochastic model, thereby completing the geological–numerical coupling.

Sensitivity analysis confirms that the repetition of lithofacies generation conditioned on the borehole data available at the main wellfields matches the stratigraphic records at 84%, indicating a high degree of geological realism. This integration will allow key parameters such as hydraulic conductivity and compressibility to be refined in a spatially consistent manner. Vertical sections extracted along stratigraphic profiles available from the literature show that the 3D static FE model reproduces the observed predominance of gravel near the Reno River and maintains the pronounced heterogeneity elsewhere

The 3D lithofacies model (version 1.0) generated in the present phase of work is publicly accessible through the SubRisk+ website (https://www.subrisk.eu/) in VTK format. The file can be readily imported into widely used scientific visualization environments, including the open-source platforms VisIt and ParaView**,** thereby ensuring transparency, reproducibility, and broad accessibility for subsequent analyses. Associated metadata consist of lithological description.

5. REFERENCES

Carle, S. F., & Fogg, G. E. (1996). Transition probability-based indicator geostatistics. *Mathematical Geology*, *28*(4), 453–476. https://doi.org/10.1007/bf02083656

Dai, Z., Ritzi, R. W., & Dominic, D. F. (2005). Improving permeability semivariograms with transition probability models of hierarchical sedimentary architecture derived from outcrop analog studies. *Water Resources Research*, *41*(7). https://doi.org/10.1029/2004wr003515

Dai, Z., Wolfsberg, A., Lu, Z., & Ritzi, R. Jr. (2007). Representing aquifer architecture in macrodispersivity models with an analytical solution of the transition probability matrix. *Geophysical Research Letters*, 34, L20406. https://doi.org/10.1029/2007GL031608

Dai, Z., Samper, J., Wolfsberg, A., & Levitt, D. (2008). Identification of relative conductivity models for water flow and solute transport in unsaturated compacted bentonite. *Physics and Chemistry of the Earth*, Parts A/B/C, 33, S177–S185. https://doi.org/10.1016/j.pce.2008.10.012

Dai, Z., Middleton, R., Viswanathan, H., Fessenden-Rahn, J., Bauman, J., Pawar, R., et al. (2014). An integrated framework for optimizing CO_2 sequestration and enhanced oil recovery. *Environmental Science & Technology Letters*, 1(1), 49–54. https://doi.org/10.1021/ez4001033

Deutsch, C. V., & Journel, A. G. (1992). GSLIB: Geostatistical Software Library. New York: Oxford University Press.

Giacomelli, S., Zuccarini, A., Amorosi, A., Bruno, L., Di Paola, G., Martini, A., Severi, P., & Berti, M. (2023). 3D geological modelling of the Bologna urban area (Italy). *Engineering Geology*, *324*, 107242. https://doi.org/10.1016/j.enggeo.2023.107242

Isotton, G., Teatini, P., Ferronato, M., Janna, C., Spiezia, N., Mantica, S., & Volonte, G. (2019). Robust numerical implementation of a 3D rate-dependent model for reservoir geomechanical simulations. *International Journal for Numerical and Analytical Methods in Geomechanics*, *43*(18), 2752–2771. https://doi.org/10.1002/nag.3000

ISPRA (Istituto Superiore per la Protezione e la Ricerca Ambientale) (2009), Geological Map of Italy 1:50000: Sheet 220 “Casalecchio di Reno”, Sheet 221 “Bologna”, and Geological Notes. https://www.isprambiente.gov.it/Media/carg/220_CASALECCHIO_DI_RENO/Foglio.html; https://www.isprambiente.gov.it/Media/carg/220_CASALECCHIO_SOTTO/Foglio.html; https://www.isprambiente.gov.it/Media/carg/221_BOLOGNA/Foglio.html; https://www.isprambiente.gov.it/Media/carg/221_BOLOGNA_SOTTO/Foglio.html.

Martelli, L., Bonini, M., Calabrese, L., Corti, G., Ercolessi, G., Molinari, F.C., Piccardi, L., Pondrelli, S., Sani, F., Severi, P. (2017). Seismotectonic Map of the Emilia-Romagna Region and Surrounding Areas, Scale 1:250,000, 2nd edn. D.R.E.AM, Firenze.

Ochoa-González, G. H., Carreón-Freyre, D., Franceschini, A., Cerca, M., & Teatini, P. (2018). Overexploitation of groundwater resources in the faulted basin of Querétaro, Mexico: A 3D deformation and stress analysis. *Engineering Geology*, 245, 192–206. https://doi.org/10.1016/j.enggeo.2018.08.014

Ritzi, R. W. (2000). Behavior of indicator semivariograms and transition probabilities in relation to the variance in lengths of hydrofacies. *Water Resources Research*, 36(11), 3375–3381

Teatini, P., Ferronato, M., Gambolati, G., & Gonella, M. (2006). Groundwater pumping and land subsidence in the Emilia-Romagna coastland, Italy: Modeling the past occurrence and the future trend. *Water Resources Research*, *42*(1). https://doi.org/10.1029/2005wr004242

Weissmann, G. S., & Fogg, G. E. (1999). Multi-scale alluvial fan heterogeneity modeled with transition probability geostatistics in a sequence stratigraphic framework. *Journal of Hydrology*, 226(1-2), 48–65. https://doi.org/10.1016/S0022-1694(99)00160-2

Ye, S., Franceschini, A., Zhang, Y., Janna, C., Gong, X., Yu, J., & Teatini, P. (2018). A novel approach to model earth fissure caused by extensive aquifer exploitation and its application to the Wuxi case, China. *Water Resources Research*, 54, 2249–2269. https://doi.org/10.1002/2017WR021872

Zhu, L., Dai, Z., Gong, H., Gable, C., & Teatini, P. (2016). Statistic inversion of multi-zone transition probability models for aquifer characterization in alluvial fans. *Stochastic Environmental Research and Risk Assessment*, *30*(3), 1005–1016. https://doi.org/10.1007/s00477-015-1089-2

Zhu, L., Franceschini, A., Gong, H., Ferronato, M., Dai, Z., Ke, Y., Pan, Y., Li, X., Wang, R., & Teatini, P. (2020). The 3-D Facies and Geomechanical Modeling of Land Subsidence in the Chaobai Plain, Beijing. *Water Resources Research*, *56*(3). https://doi.org/10.1029/2019wr027026

Zuccarini, A., Giacomelli, S., Severi, P., & Berti, M. (2024). Long-term spatiotemporal evolution of land subsidence in the urban area of Bologna, Italy. *Bulletin of Engineering Geology and the Environment*, *83*(1), 35. https://doi.org/10.1007/s10064-023-03517-5